

## 2D SURFACE QUASI GEOSTROPHIC EQUATIONS AND ITS REGULARITY, A NUMERICAL STUDY

PAWAN SHRESTHA <sup>1</sup> AND DURGA JANG KC <sup>2</sup> AND RAMJEE SHARMA<sup>3</sup>

<sup>1,2</sup> *Central Department of Mathematics, TU*

<sup>3</sup> *University of North Georgia, USA*

*Corresponding Author: Durga Jung KC, email: durgajkc@gmail.com*

**Abstract:** In this article, we present some results on the numerical solutions of the 2-D Surface Quasi Geostrophic Equation (SQG) using pseudospectral method along with an exponential filter. The global regularity of solution of inviscid SQG equation for general data remains an outstanding open problem. Our computations mainly focus on the inviscid and supercritical cases. We monitored the regions where the level curves come significantly close to one another, the  $L^2$  norm and the growth of  $|\nabla^\perp \theta|$  throughout our computations. Our numerical findings show that there is no significance difference among the solutions of the super critical, critical and subcritical cases as we vary the values of the parameter  $\alpha$  in the interval  $(0, 1)$ .

**Key Words:** SQG equations, Inviscid, Dissipative, Global regularity, Finite Time singularity

**AMS (MOS) Subject Classification.** 35Q35.

### 1. INTRODUCTION

The two dimensional (2D) Surface Quasi Geostrophic (SQG) equation is given by

$$(1.1) \quad \begin{aligned} \partial_t \theta + u \cdot \nabla \theta + \kappa (-\Delta)^\alpha \theta &= 0 \\ \nabla \cdot u &= 0 \\ \theta(x, 0) &= \theta_0(x) \end{aligned}$$

where  $\kappa \geq 0$  and  $\alpha > 0$  are parameters,  $\theta = \theta(x_1, x_2, t)$  is a scalar representing the potential temperature and  $u = (u_1, u_2)$  is the velocity field determined from  $\theta$  by the stream function  $\psi$  with the auxiliary relations

$$\begin{aligned} (u_1, u_2) &= (-\partial_{x_2} \psi, \partial_{x_1} \psi), \\ (-\Delta)^{1/2} \psi &= \theta. \end{aligned}$$

Assuming  $\Lambda = (-\Delta)^{1/2}$  and  $\nabla^\perp = (-\partial_{x_2}, \partial_{x_1})$ , the above relation can be written as

$$u = \nabla^\perp \Lambda^{-1} \theta = (-R_2 \theta, R_1 \theta)$$

where  $R_1$  and  $R_2$  are the usual Riesz transforms. The periodic box  $T^2$  or  $\mathbb{R}^2$  is the domain considered. Depending upon  $\kappa$  and  $\alpha$ , the equation can be divided into the following categories:

- (1) When  $\kappa = 0$ , the equation (1.1) is called the inviscid SQG equation.
- (2) When  $\kappa > 0$ , the equation (1.1) is called the dissipative SQG equation.

- (a) When  $\alpha > \frac{1}{2}$ , the equation (1.1) is called the subcritical SQG equation.
- (b) When  $\alpha = \frac{1}{2}$ , the equation (1.1) is called the critical SQG equation.
- (c) When  $\alpha < \frac{1}{2}$ , the equation (1.1) is called the supercritical SQG equation.

J.G. Charney derived the general 3D quasi geostrophic equations in 1940's. These equations are useful to describe major features of motions in the atmosphere and oceans in the midlatitudes [10]. The SQG equation is the particular case of 3D geostrophic equations with uniform vorticity. This SQG equation models the evolution of buoyancy or the potential temperature on the 2D horizontal boundaries. The inviscid SQG equation is useful in modeling the atmospheric phenomenon such as frontogenesis, the formation of strong fronts between the masses of hot and cold air. Also, the inviscid SQG is an important example of an active scalar and important testbed for turbulence theories due to some of its distinctive features [8, 24]. In the geophysical studies of strongly rotating fluids [3, 10] the SQG equation with  $\alpha = \frac{1}{2}$  is arose.

The authors in [12, 17, 23] showed that  $L^2$ - weak solutions are global in time and the physically reasonable solution are at least local in time . Also, the classical solution exhibit certain geometric configuration which do not develop the finite time singularities [4, 5, 6]. The global regularity for the general initial data is still open.

For the subcritical case  $\alpha > \frac{1}{2}$ , the dissipation term is sufficient to control the nonlinearity and global regularity is a consequence of an a priori bound [18, 23]. For the critical case  $\alpha = \frac{1}{2}$ , the global regularity issue is more delicate. The authors established the global regularity of the classical solutions together with  $L^\infty$  data comparable to  $\kappa$  in [21]. The global regularity for the general data was obtained in [2] for the periodic case while in [15] for the whole space. Wu [13] established global regularity results for the regularized models with critical or subcritical indices. He extended the notion of dissipative solution of Duchon and Robert [9] to the weak solution of the quasi geostrophic equations[13] on the basis of proof of Onsager's conjecture [16] related with weak solutions of 3D Euler equations.

The information for the supercritical case  $\alpha < \frac{1}{2}$  is partially known to the present situation. The work in [7, 19, 20] imply that the solution of supercritical SQG equation can develop a finite time singularity in the regularity window between  $L^\infty$  and  $C^\delta$  with  $\delta < 1 - 2\alpha$ . By using maximum principle, the authors in [1] proved the local existence and global results for small initial data for the supercritical case of dissipative 2D Quasi-geostrophic equations.

Constantin, Majda and Tabak [17], in 1994, performed the numerical experiments on a  $2\pi$ -periodic box and predicted strong front formation and potential singular behavior of the solutions of the SQG equation in the inviscid case. They monitored two physical quantities, kinetic energy and the pseudo energy. They used finer partitions ranging from  $256^2$  to  $512^2$  to  $1024^2$  with the following three types of initial data.

- (1)  $\theta(x, 0) = \sin x_1 \sin x_2 + \cos x_2$
- (2)  $\theta(x, 0) = -(\cos 2x_1 \cos x_2 + \sin x_1 \sin x_2)$
- (3)  $\theta(x, 0) = \cos 2x_1 \cos x_2 + \sin x_1 \sin x_2 + \cos 2x_1 \sin 3x_2$ .

The first initial condition is the simplest smooth data showing the nonlinear behavior and is the combination of two lowest eigenmodes.

The first data set involves a hyperbolic saddle in the initial level sets of temperature in the regime of strong nonlinear behavior. The numerical solutions indicate strong nonlinear front formation and potentially singular behavior. The second data set involves the elliptic level sets in  $\theta$  and the numerical solutions asserts that the solution behaves nonlinearly as in the first set initially but self consistently saturates to exponential growths of gradients without singular behavior. In the third data set, there is robust feature of strong front formation. They concluded that

“if the geometry of level sets of the active scalar is simple and does not contain a hyperbolic saddle in the region of strongly nonlinear behavior, then no singular behavior is possible” [17]. Figure 1 shows the evolution of level sets and 3D surface plot of the type (3) data.

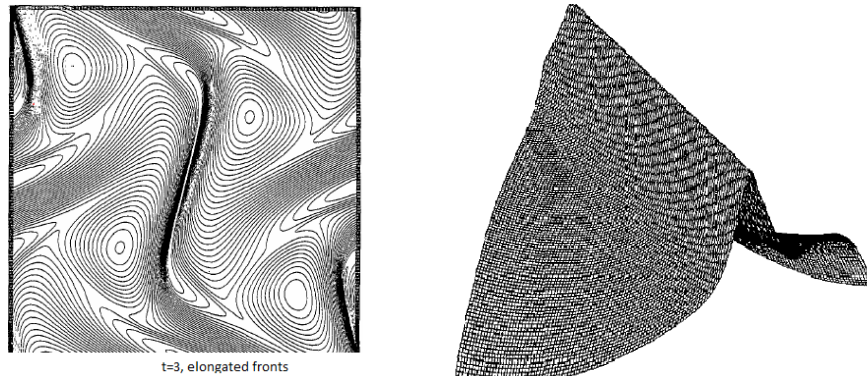


FIGURE 1. Contour plot and Nature of front

Based on the simple initial condition used in [17], the authors in [14] proposed that the temperature gradient can be fitted equally well by a double-exponential function of time rather than an algebraic blow up. Also for the viscous case, with series of computations and different Reynolds numbers, they found that the critical time at which the temperature gradient attains the first local maximum depends double logarithmically on the Reynolds numbers, which suggests the global regularity of the inviscid flow.

Constantin, Sharma, Wu et. al in [22] used pseudospectral method with an improved exponential filter to extend the computations in [17] using the same initial data sets. Their computations revealed the nature of solutions for a longer time interval without noticing any singularities in the solutions. To increase the speed and accuracy of the computations, the pseudospectral algorithm was parallelized by the slab decomposition. About time  $t = 7.5$ , strong hyperbolic saddle front was observed as in [17]. If further continued then there was

steep antiparallel double front and maximum gradient continues to grow up about  $t = 13.5$ . After that gradient starts to decay and there was absence of strong fronts. One of the graphs for the gradient growth is presented in Figure 2.

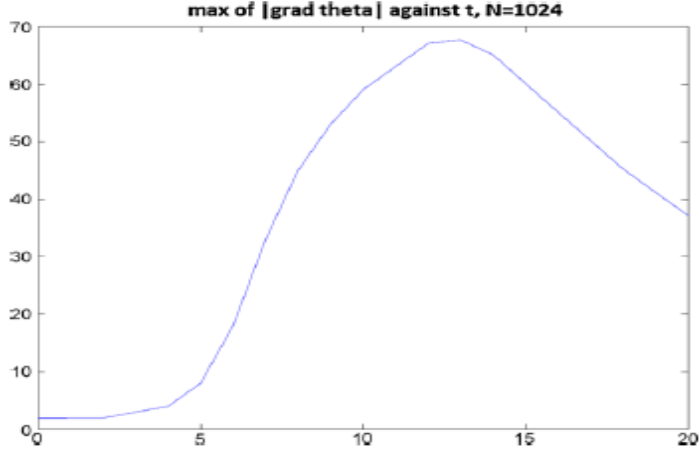


FIGURE 2. Gradient growth

The issue of development of a finite time singularity in the solutions of the 2D SQG equations in the supercritical and inviscid cases is still open. Motivated by the work in [17] and [22], we performed a series of numerical simulations to compute the solutions to extend the previous results for the longer time period by using the 2/3 dealiasing rule. Details of the method are explained in Section 2. The numerical results are presented graphically and explained in Section 3. Section 4 concludes the paper.

## 2. NUMERICAL METHOD

The numerical method for the computation is described in the section. We use pseudospectral method for this problem because of periodic boundary condition.  $\tilde{\theta}$  approximates the solution  $\theta$  which is given by the relation

$$\tilde{\theta}(x, t) = \sum_{k_1, k_2 = -\frac{N}{2}}^{\frac{N}{2}-1} \hat{\theta}(k_1, k_2) e^{ikx}$$

where  $\hat{\theta}$  denotes the Fourier transform of  $\theta$  and is given by

$$\hat{\theta}(k_1, k_2) = \frac{1}{(2\pi)^2} \int_{T^2} \theta(x_1, x_2) e^{-i(k_1 x_1 + k_2 x_2)} dx_1 dx_2.$$

Here  $N$  is a fixed number. Also, taking the Fourier transform of the SQG equation, we obtain

$$\partial_t \widehat{\theta}(k) = -ik_1 \widehat{(u_1 \theta)}(k) - ik_2 \widehat{(u_2 \theta)}(k) - 2\pi\kappa |k|^{2\alpha} \hat{\theta}(k)$$

where  $k = (k_1, k_2)$  is the wave number and  $k_1, k_2 = -\frac{N}{2}, \dots, \frac{N}{2} - 1$ . The velocity field  $u$  given by

$$\hat{u}(k) = i \frac{(-k_2, k_1)}{|k|} \hat{\theta}(k)$$

which is computed in the Fourier space.

Pseudospectral methods have the advantage of computing a nonlinear convection term very efficiently using the Fast Fourier Transform. The product  $u_1\theta$  and  $u_2\theta$  are computed in the physical space. The resulting equation becomes  $\partial_t \hat{\Theta} = A\hat{\Theta}$  where  $\Theta$  is the matrix with the modes of  $\theta$  as its entry and  $A$  is a  $N \times N$  matrix whose entries are obtained from the Fourier transform. The time integration is carried out through fourth order Runge-Kutta method.

To reduce the aliasing error, we used the exponential filter instead of the traditional 2/3 dealiasing rule. While using an exponential filter, the Fourier multiplier  $ik_j$  for the differential operator  $\frac{\partial}{\partial x_j}$  is replaced by  $ik_j\phi(|k_j|)$ , where  $\phi(k) = e^{-\alpha(\frac{k}{N})^{m_f}}$  for  $|k| \leq N$ . Here  $N$  is the numerical cutoff for the Fourier modes, and  $m_f$  is the order of the filter. The value of  $\alpha$  is chosen so that  $\phi(N) = e^{-\alpha} = \text{machine precision}$ . For a smooth function  $f(x)$ , we have  $\|f(x) - D_N f(x)\| = O(N^{-m_f})$  where  $D_N f = F^{-1}(ik\phi(|k|) - F(f))$  is the numerical approximation of  $f'(x)$  and  $F$  denotes the Fourier transform operator. The improved exponential filter used in our computation is shown in Figure 3.

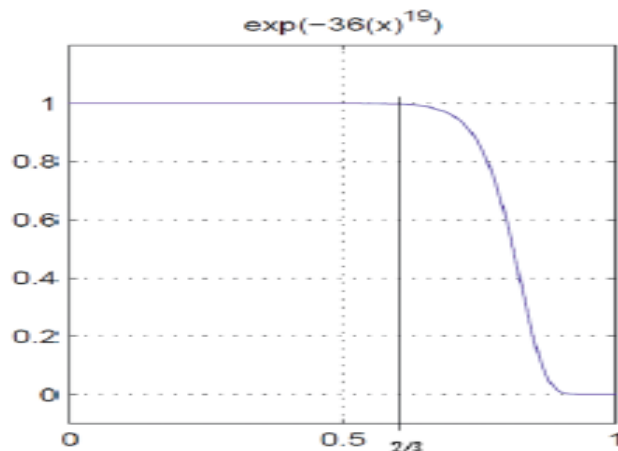


FIGURE 3. Exponential filter

While in the case of 2/3 dealiasing rule, last 1/3 of the high frequency are set to zero and the first 2/3 of the Fourier modes are unchanged. As a particular instance, the interval  $[-\frac{N}{2}, \frac{N}{2}]$  is considered in which  $[-\frac{N}{3}, \frac{N}{3}]$  is taken and the two intervals  $[-\frac{N}{2}, -\frac{N}{3}]$  and  $[\frac{N}{3}, \frac{N}{2}]$  are avoided.

We investigated the existence of development of any finite time singularity and monitored their large time behavior. To study this, we closely examined the evolution of the level curves of  $\theta$  and the growth of  $\nabla\theta$  at various times, and tried to identify the potential time at which the most singular behavior could occur in the solutions. In this regard, mathematical criterion given by [17] is used to characterize how the smooth solution of the equation

$$(2.1) \quad \frac{D\theta}{Dt} = \frac{\partial\theta}{\partial t} + v \cdot \nabla\theta = 0$$

can be singular. This is the simplest type which is analogous to characterize the singular solution of 3D Euler equation [11], and can be stated as:

"The time interval  $[0, T^*]$  with  $T^* < \infty$  is a maximal interval of a smooth solution for the 2D quasi geostrophic active scalar if and only if  $\int_0^T |\nabla\theta|_{L^\infty}(s)ds \rightarrow \infty$  as  $T \rightarrow T^*$  with norm  $|f|_{L^\infty} = \max_{x \in R^2} |f(x)|$ " [17].

It is a well known fact that the  $L^2$  norm of the solution of the inviscid case is preserved. To establish the validity of our numerical solutions, we monitored the  $L^2$  norms throughout of our computations.

### 3. NUMERICAL RESULTS

We performed our numerical experiment to reveal the behavior of the solution at critical index for the dissipative and inviscid SQG equations using the same initial conditions as given above. We investigated if the solutions could develop any finite time singularity and examined their large time behavior. To study this, we closely examined the level curves of  $\theta$  at various times and tried to identify the time at which the most singular behavior could occur in the solutions. To validate our numerical results, we continuously monitored the value of  $L^2$ -norm of  $\theta$  throughout our computations and made sure that the norm is conserved.

**3.1. Inviscid SQG Equation.** In our computations, we observed that the  $L^2$ -norm continued to decrease with time, whereas the  $L_\infty$ -norm decreased up to  $t = 8$  and, increased until  $t = 10$ , and again decreased until  $t = 12$ . This rise and fall were observed up to  $t = 16$ . Also, we monitored the growth of the  $L_\infty$ -norm of  $\nabla\theta$ . We observed that its value increased continuously up to  $t = 10$ , decreased up to  $t = 12$ , and then continuously increased up to  $t = 15$ . We also monitored the power spectra at various times to make sure that the larger modes are well resolved as shown in the following Figures 4, 5, 6 7.

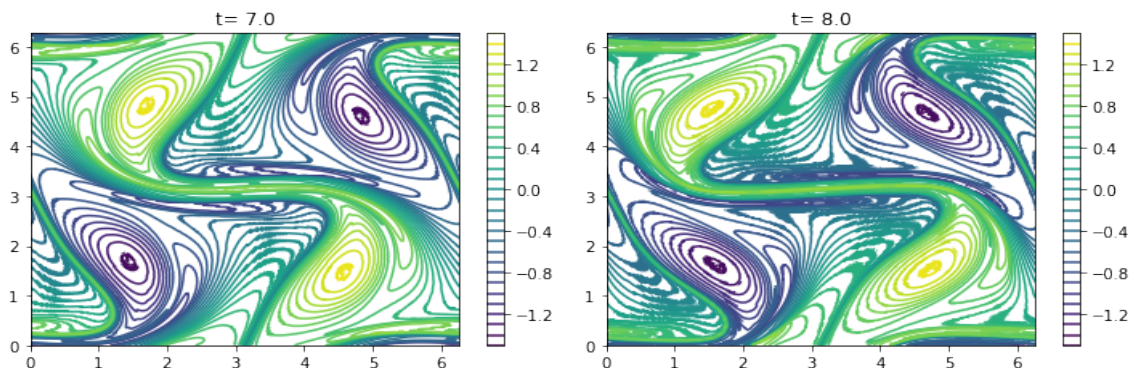


FIGURE 4. Plots at  $t=7$  and  $t=8$  for inviscid SQG equation

**3.2. Dissipative SQG Equations.** In the dissipative case, the analytical results for the subcritical and critical cases have been already obtained [17]. So, we focused our computations to supercritical case as no analytical solutions have been obtained until now. We also performed our computation using the same initial condition as with the inviscid case above. Our computations showed the similar results for the  $L^2$  norm and  $L_\infty$  norm as with the inviscid case. We observed that the  $L^2$ -norm continued to decrease throughout our

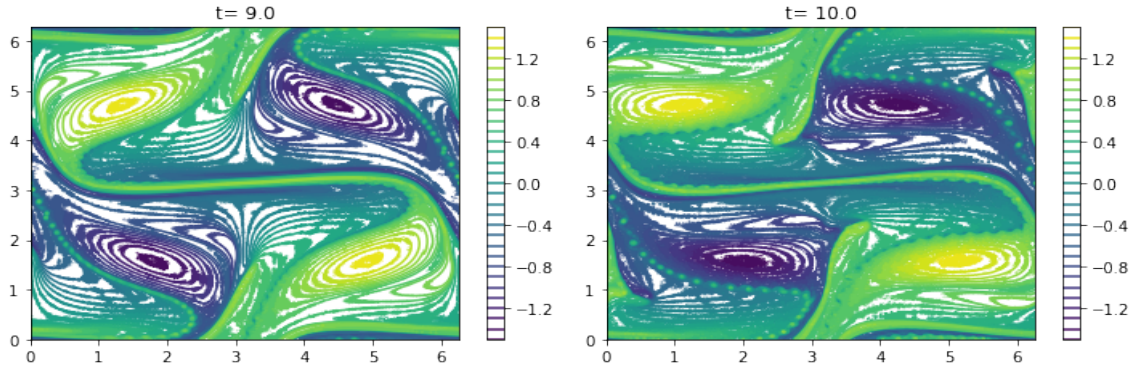


FIGURE 5. Plots at  $t= 9$  and  $t= 10$  for inviscid SQG equation

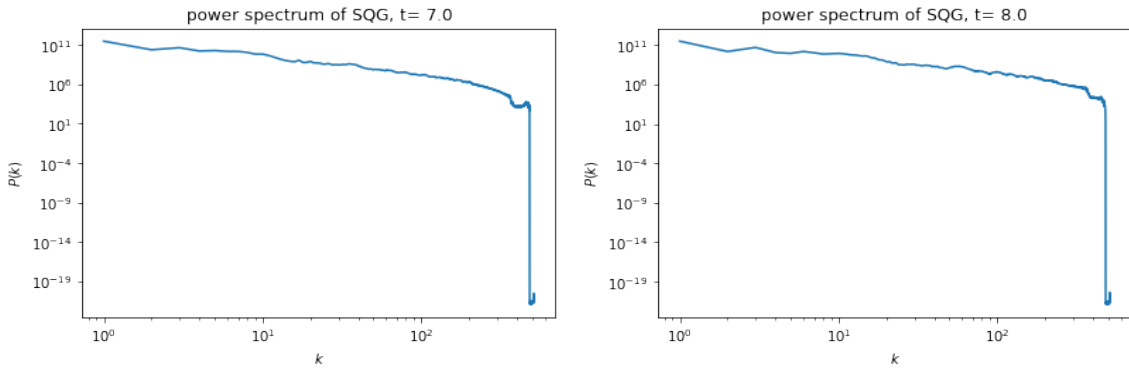


FIGURE 6. Plots at  $t= 7$  and  $t= 8$  of Power Spectrum for inviscid SQG equation

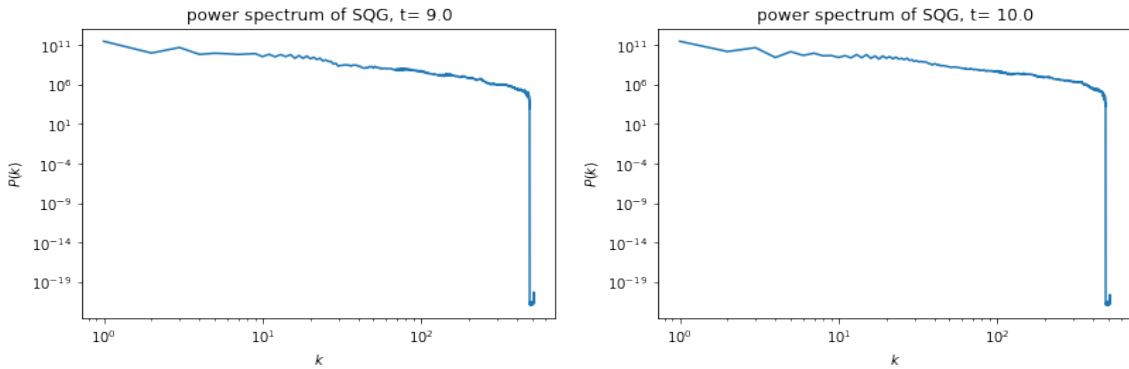
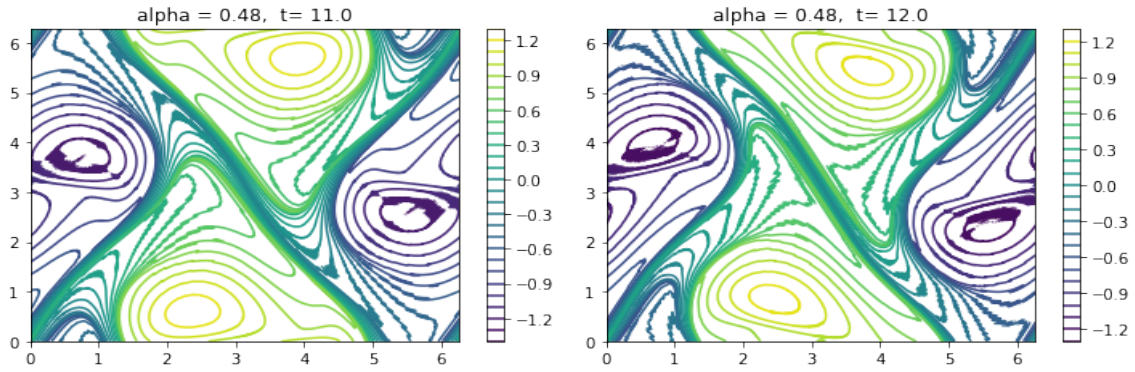
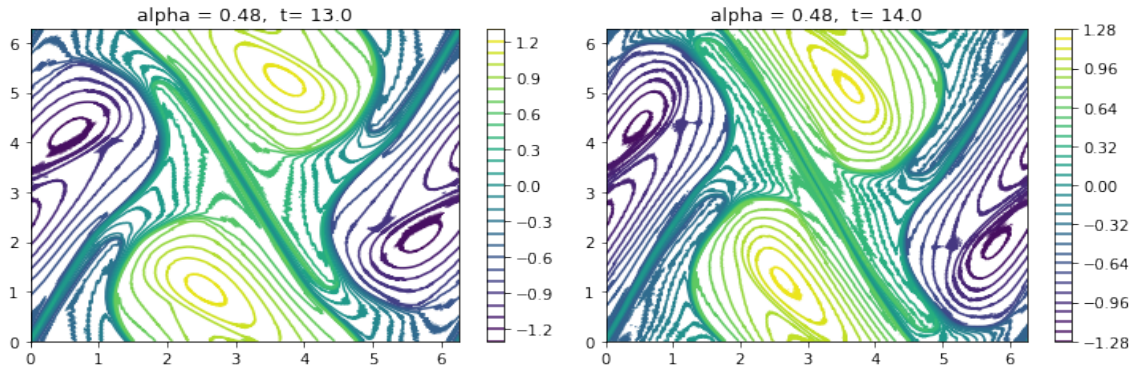
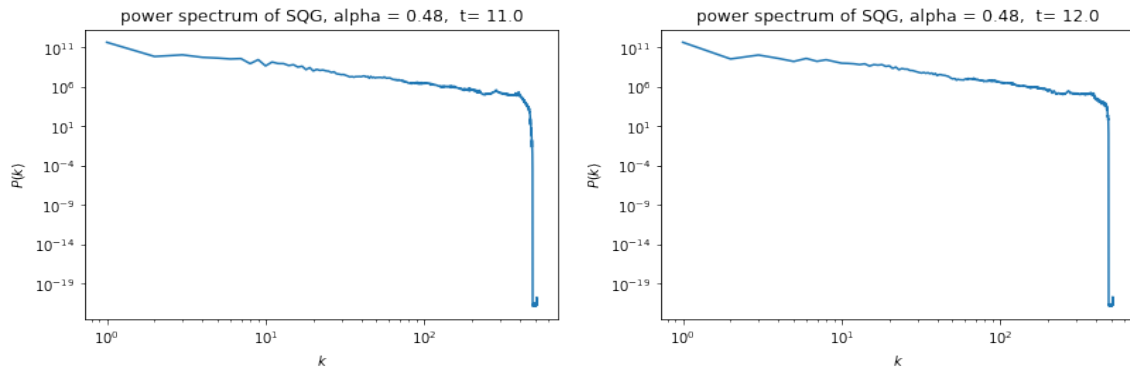


FIGURE 7. Plots at  $t= 9$  and  $t= 10$  of Power Spectrum for inviscid SQG equation

computation, whereas the  $L_\infty$ -norm decreased up to  $t = 8$ , increased up to  $t = 10$ , and again decreased up to  $t = 12$ . This rise and fall in the values were observed up to  $t = 16$ . Similarly, the value of  $L_\infty$ -norm of  $\nabla\theta$  increased continuously up to  $t = 10$ , decreased up to  $t = 12$ , and then continuously increased up to  $t = 15$ . We also noticed that this value sharply increased at  $t = 10$  and then sharply fell at  $t = 11$  but the reason behind this is not clear at this time and it needs further investigation. Our findings are presented in the following Figures 8, 9, 10, 11.

Tables 1 and 2 show the values of  $L^2$ -norm in the inviscid and dissipative cases.

FIGURE 8. Plots at  $t=11$  and  $t=12$ FIGURE 9. Plots at  $t=13$  and  $t=14$ FIGURE 10. Power Spectrum at  $t=11$  and  $t=12$ 

|         |            |            |            |            |            |
|---------|------------|------------|------------|------------|------------|
| $t$     | 1          | 2          | 3          | 4          | 5          |
| L2-norm | 110.851252 | 110.851252 | 110.850575 | 110.839593 | 110.797750 |
| $t$     | 6          | 7          | 8          | 9          | 10         |
| L2-norm | 110.730007 | 110.651406 | 110.594932 | 110.510071 | 110.466472 |

TABLE 1. Value of  $L^2$ -norm of Inviscid case

From the above tables, we see that the  $L^2$  norm is conserved in the inviscid case as there is no viscosity. On the other hand, in the dissipative case the value of  $L^2$ -norm decreases constantly and energy dissipates continuously which is due to the viscosity.

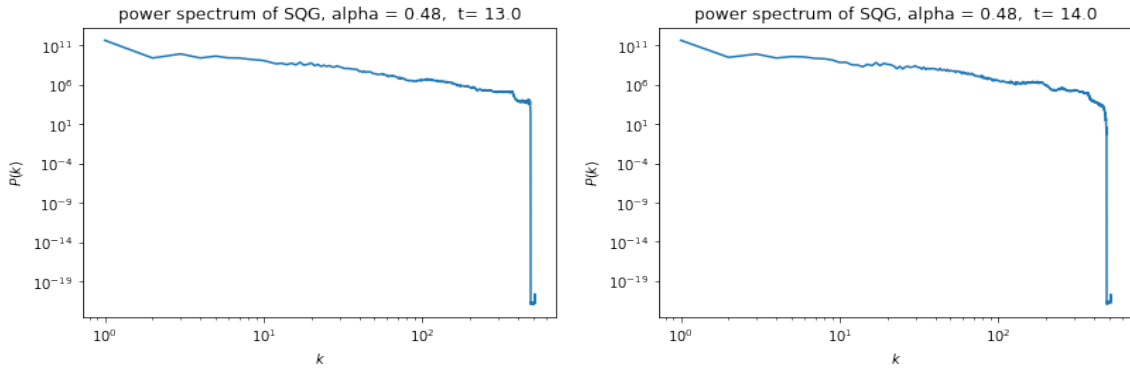


FIGURE 11. Power Spectrum at t=13 and t=14

|         |            |            |            |            |            |
|---------|------------|------------|------------|------------|------------|
| t       | 1          | 2          | 3          | 4          | 5          |
| L2-norm | 109.377354 | 107.916750 | 106.464917 | 105.009819 | 103.534279 |
| t       | 6          | 7          | 8          | 9          | 10         |
| L2-norm | 102.039835 | 100.544520 | 99.060618  | 97.581038  | 96.097118  |

TABLE 2. Value of  $L^2$ -norm of Dissipative case for kappa=0.01

#### 4. CONCLUSION

We performed numerical computations to study the evolution of solutions of the SQG equation for the inviscid and dissipative cases. We were able to pursue our computations beyond the previously recorded time. For the inviscid case, our computational results confirmed that the inviscid equation develops a strong hyperbolic saddle front at about  $t = 7$  as previously observed in [17]. We further observed that the gradient of theta continues to grow up and decay up to  $t = 15$ , and finally no regeneration of strong fronts occurs. In this case, our computations show that the  $L^2$ - norm is conserved. We performed our computation for the dissipative case beyond the previously recorded time. The computations have been carried out for the long time behavior in the neighborhood of  $\alpha = \frac{1}{2}$  and no drastic change in nature of the solution is noticed. Moreover, it is also observed that  $L^2$ -norm vanishes at a constant rate for the dissipative case.

#### 5. ACKNOWLEDGMENT

We acknowledge the Nepal Academy of Science and Technology(NAST) for the fellowship and Central Department of Mathematics, TU.

#### REFERENCES

- [1] A. Cordoba, D. Cordoba, A maximum principle applied to quasi geostrophic equations, *Commun.Math. Phys.*, Vol. 249, pp 511-528, 2004
- [2] A. Kiselev, F. Nazarov, and A. Volberg, A.: Global wellposedness for the critical 2d dissipative quasi-geostrophic equation, *Invent.Math.*, Vol.167, pp 445-453, 2007
- [3] A. Majda and E. Tabak, A two dimensional model for quasi geostrophic flow: comparison with the two dimensional Euler flow, *physica*, Vol. 98, pp 515-522, 1996

- [4] D. Chae, The geometric approaches to the possible singularities in the inviscid fluid flows, *J. Phys.A.*, Vol. 41, 2008
- [5] D. Cordoba, C. Fefferman, Scalars convected by a two dimensional incompressible flow, *Commun. Pure Appl. Math.*, Vol.55, pp 255-260, 2002
- [6] D. Cordoba, C. Fefferman, On the behavior of several two dimensional fluid equations in singular scenarios, *Proc. Natl.Acad.Sci*, Vol.98, pp 4311-4312, 2001
- [7] H. Dong, N. Pavlovic, A regularity criterion for the dissipative quasi-geostrophic equation, *Anal.Non Lineaire*, Vol. 26, pp 1607-1619, 2009
- [8] I. Held, R. Pierrehumbert, S. Garner, K. Swanson: Surface quasi-geostrophic dynamics, *J. Fluid Mech.*, Vol.282, pp 1-20, 1995
- [9] J. Duchon, R. Robert, Inertial energy dissipation from weak solutions of incompressible Euler and Navier-Stokes equations, *Nonlinearity*, Vol.13, pp 249-255, 2000
- [10] J. Pedolsky, Geophysical Fluid Dynamics, Springer, NewYork,1987
- [11] J.T. Beale, T. Kato, A. Majda, Remarks on breakdown of smooth solutions for 3D Euler equations, *Communication in Mathematics and Physics*, Vol.94, pp 61-66, 1984
- [12] J. Wu, Solutions of 2-D quasi-geostrophic equation in a Holder spaces, *Nonlinear Anal*, Vol. 62, pp 579-594, 2005
- [13] J. Wu, The quasi geostrophic equations and its two regularizations, *Commun. Partial Differential Equations*, Vol. 27, pp 1161-1181, 2001
- [14] K. Ohkitani and M. Yamada, Inviscid and inviscid-limit behavior of a surface quasi-geostrophic flow, *Physics of Fluids*, Vol. 9, pp 876-882, 1997
- [15] L. Caffarelli, A. Vasseur, Drift diffusion equations with fractional diffusion and quasi geostrophic equations, *Annals of Mathematics Second Series*, Vol. 171, pp 1903-1930, 2010
- [16] L. Onsager: Statistical Hydrodynamics, *Nuovo Cim. Suppl.*, Vol.6, pp 279-289, 1949
- [17] P. Constantin, A. Majda, E. Tabak, Formation of strong fronts in the 2 D quasi-geostrophic thermal active scalar, *Nonlinearity*, Vol. 7, pp 1495-1533, 1994
- [18] P. Constantin, J. Wu, Behavior of solutions of 2D quasi geostrophic equations, *SIAM J. Math.Anal.*, Vol.30, pp 937-948, 1999
- [19] P. Constantin, J. Wu, Regularity of Holder continuous solutions of the supercritical quasi geostrophic equation, *Annales of Institute of Henri Poincare* , Vol.25, pp 1103-1110, 2008
- [20] P. Constantin, J. Wu, Holder continuity of solutions of the supercritical dissipative hydrodynamic transport equation, *Annales of Institute of Henri Poincare*, Vol. 26, pp 159-180, 2009
- [21] P. Constantin, D.Cordoba, J. Wu, On the critical dissipative quasi geostrophic equation, *Indiana Univ. Math.J.*, Vol. 50, pp 97-107, 2001
- [22] P. Constantin, M. Lai, R. Sharma, Y. Tseng, J. Wu, New numerical results for the surface quasi geostrophic equation, *J.Sci Comput.*, Vol. 50, pp 1-28, 2012
- [23] S. Resnick, Dynamical problems in a nonlinear advective partial differential equations, Ph.D. thesis, University of Chicago, 1995
- [24] W. Blumen, Uniform Potential vorticity flow, Part I Theory of wave interactions and two dimensional turbulence, *J.Atoms. Sci.*, Vol. 35, pp 774-783, 1978